Available online at www.sciencedirect.com
SCIENCE DIRECT®
Journal of Catalysis 224 (2004) 138–147
JOURNAL OF CATALYSIS
www.elsevier.com/locate/jcat

DBT derivatives adsorption over molybdenum sulfide catalysts: a theoretical study

Sylvain Cristol,[a,*] Jean-François Paul,[a] Edmond Payen,[a] Daniel Bougeard,[b] François Hutschka,[c] and Sylvain Clémendot[c]

[a] *Laboratoire de Catalyse de Lille, CNRS/UMR 8010, Bâtiment C3, Université des Sciences et Technologies de Lille, F-59655 Villeneuve d'Ascq cedex, France*
[b] *Laboratoire de Spectroscopie Infra-Rouge et Raman, CNRS/UPR 2631, Bâtiment C5, Université des Sciences et Technologies de Lille, F-59655 Villeneuve d'Ascq cedex, France*
[c] *Total, CERT, BP 27, F-76700 Harfleur, France*

Received 15 October 2003; revised 28 January 2004; accepted 3 February 2004

Abstract

We report density-functional calculations of dibenzothiophene and dimethyldibenzothiophene over different molybdenum sulfide surfaces representing the active sites of the simplest hydrodesulfurization catalysts. Using the adsorption energies and geometries of the molecules on the different sites, we propose an interpretation of the catalytic activities and selectivities published in the literature, which demonstrated the existence of two parallel reaction mechanisms. Among the various possible configurations, η^1(S) adsorption on the sulfur edge of the active phase seems to be at the origin of the direct desulfurization of the molecules whereas benzene ring adsorption on the molybdenum edge is at the origin of the hydrogenation pathway. Although a combination of aromatic and steric effects strongly inhibits its adsorption, we show that the presence of stacking defects on the molybdenum sulfides would allow the adsorption and the activation of DMDBT.

Keywords: Catalysis; Hydrodesulfurization (HDS); Molybdenum sulfide (MoS_2); Dibenzothiophene (DBT); Dimethyldibenzothiophene (DMDBT); Density-functional theory (DFT)

1. Introduction

The new environmental regulations in most of the developed countries will impose the reduction of the sulfur compounds (SO_x) produced upon fuel combustion [1]. This will imply the production of cleaner fuels and thereby an improvement of the efficiency of the hydrodesulfurization (HDS) of the petroleum feedstock. This reaction is performed industrially on $CoMo/Al_2O_3$ or $NiMo/Al_2O_3$ catalyst. Their active phase consists of MoS_2 nanocrystallites well dispersed on a high-surface-specific alumina and promoted by cobalt or nickel atoms [2,3]. These catalysts work reasonably well for the actual diesel specifications; however, the residual sulfur level in the gas oil is due to the presence of polyaromatic sulfide derivatives that are not desulfurized under the classical HDS conditions. Those refractory compounds are mainly dibenzothiophene (DBT) derivatives, especially those alkylated in 4 and/or 6 positions like 4,6-dimethyldibenzothiophene (DMDBT) [4–7]. Understanding the reactivity of those molecules is mandatory in order to develop new active phases that will be active for deep desulfurization of gas oils and to match the new environmental specification.

Many studies have been devoted to the hydrodesulfurization mechanisms of those molecules. They all agree that there are two possible reaction pathways as shown in Fig. 1 [8–11]. The first one is called the direct desulfurization (DDS) and produces biphenyl (BP) and its methylated derivative for DBT and DMDBT desulfurization, respectively. The second, usually called the hydrogenative pathway (HYD), involves the hydrogenation of one of the benzene rings before desulfurization yielding cyclohexylbenzene (CHB) or its dimethylated derivative in the case of DMDBT desulfurization. The contribution of BP hydrogenation to the production of CHB has been shown to be negligible [12]. The ratio between the two reaction paths depends on both the nature of the molecule and the catalyst.

* Corresponding author.
E-mail address: sylvain.cristol@univ-lille1.fr (S. Cristol).

0021-9517/$ – see front matter
doi:10.1016/j.jcat.2004.02.008

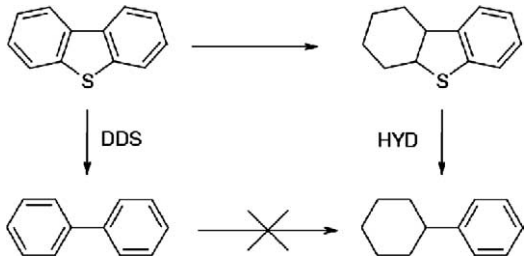

Fig. 1. Hydrodesulfurization reaction paths of DBT and its derivatives.

It is now well admitted that the active sites are coordinately unsaturated sites (CUS) located at the edges of the disulfide nanocrystallites [13]. From a crystallographic point of view, these edges correspond to the (100) surface that present two types of termination: one exposing unsaturated molybdenum atoms (hereafter called molybdenum edge), the other one exposing sulfur atoms (called sulfur edge). This order is valid for the more widely considered hexagonal phase. A rhombohedral MoS_2 phase also exists for which the (100) surface exposes only molybdenum edges and the (-100) surface will expose only sulfur edges. This kind of crystal termination is not considered in our model and we do not think that it would imply strong differences as the different layers are quite independent from an electronic point of view. Although the surface states of both the promoted and the unpromoted MoS_2 active phase have been widely studied theoretically [14–18], there are very few studies about the interaction of sulfur-containing molecules with these catalytic phases. Furthermore, they mainly deal with thiophene [19,20] or benzothiophene [21]. The fact that those molecules are good models for deep HDS catalysis is highly questionable as DBT and DMDBT have properties such as aromaticity and size that are not reproduced in those model molecules. Only very recently, Yang et al. [22] reported a density-functional study of the adsorption of various methylated DBT derivatives on a MoS_2 cluster. These authors show very interesting differences between substituted and nonsubstituted molecules; however, they only consider the adsorption on a clean molybdenum edge of the cluster. Previous theoretical studies have shown, in agreement with spectroscopic characterization, that such a situation is not realistic and that the surface state is much more complex [23,24]. Furthermore, the sulfur edge of the molybdenum disulfide crystallites should also be taken into account, as there is no experimental evidence that one edge is more important than the other in HDS catalysis. In this paper we present an ab initio theoretical study of the adsorption of both DBT and DMDBT on a more realistic model surface, taking into account the sulfur coverage of both edges of the surface of the active phase.

2. Computational methods

The density-functional theory (DFT) calculations were performed with the Vienna ab initio simulation package (VASP) [25–28], which is based on Mermin's finite temperature DFT [29]. The wavefunction is expanded in a plane wave basis set and the electron–ion interactions are described using optimized ultrasoft pseudopotentials [30,31]. The resolution of the Kohn–Sham equations is performed using an efficient matrix diagonalization routine based on a sequential band by band residual minimization method for the one-electron energies. The optimization of the atomic positions is performed via a conjugate gradient minimization of the total energies using the Hellmann–Feyman forces on the atoms.

Throughout this work, we used a large supercell ($20.0 \times 9.48 \times 18.44$ Å^3) containing three unit cells in the y direction, four in the x direction, and three layers along the z axis. The two upper rows in the x direction are allowed to relax as well as the adsorbed molecule, while the atoms of the two lower ones are kept fixed at their optimized bulk positions in order to simulate bulk constraints. The calculations were performed at Γ point with a cutoff energy of 210 eV and a Methfessel–Paxton smearing with $\sigma = 0.1$ eV. The exchange correlation was treated using the functional of Perdew and Zunger [32] and the generalized gradient approximation of Perdew et al. [33].

3. Sulfur coverage and catalytic sites

Apart from the basal (001) plane which is known to be inactive in catalysis, the crystallites alternatively expose as noted earlier two type of edges: the $(10\bar{1}0)$ and the $(\bar{1}010)$ edge. The former is, in its perfect crystallographic termination, constituted of sulfur atoms, the latter exposing unsaturated molybdenum atoms. As industrial conditions involve the presence of both H_2 and H_2S in the gas phase, the (100) surface could be sulfur rich or sulfur deficient. Indeed, H_2S can depose a sulfur atom on an unsaturated molybdenum atom. On the other hand, H_2 can react with surface sulfur atoms to create a vacancy and produce H_2S. We thus have to consider the following equilibrium:

$$\text{Surface–S} + H_2 \rightleftharpoons \text{Surface} + H_2S.$$

The energy of each sulfur addition and each sulfur removal has been computed [17,21,34], and the stability of each surface has been deduced. These calculations showed that the most stable surface is obtained by adding three sulfur atoms on the molybdenum edge of the perfect crystallographic surface as shown in Fig. 2a. The overstoichiometric sulfur atoms are adsorbed in a bridging position between two molybdenum atoms. Such a geometry leads to a coordination number of six for the molybdenum atoms and two for the sulfur atoms. The high stability of this structure comes from the saturation of all the surface molybdenum atoms with sulfur atoms. This saturation also implies that the adsorption of large molecules such as DBT and DMDBT is impossible on this stable surface. We thus have to create vacancies on this surface. Numerous CUS can be created on both edges of the

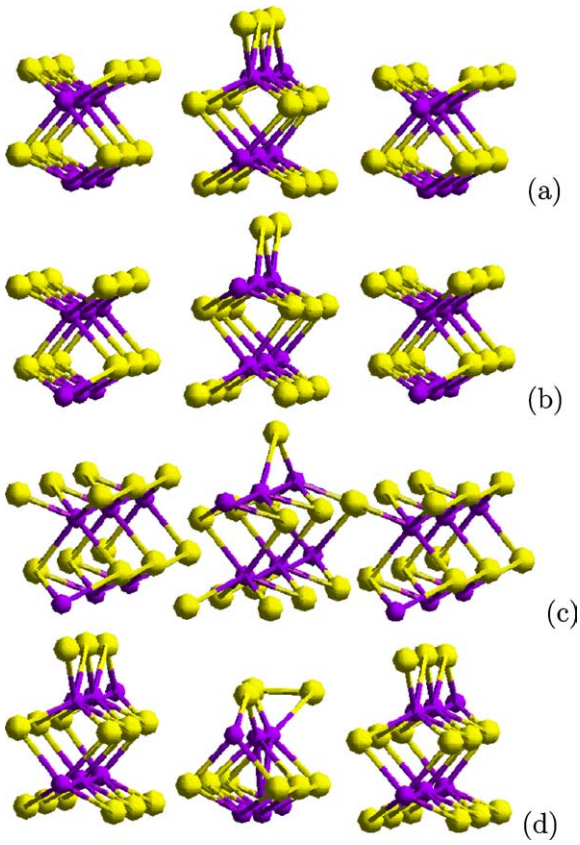

Fig. 2. The MoS_2(100) surface. (a) Most stable surface. (b) Site 1. (c) Site 2. (d) Site 3.

MoS_2(100) surface, but we have chosen the three more stable ones as they are more likely to appear under the catalytic conditions.

The first potential active site we consider (site 1) is a single vacancy on the metallic edge of the most stable surface (Fig. 2b). On this site, two molybdenums are pentacoordinated. Its creation energy is 1.3 eV. The second one (site 2) is obtained by removing a second sulfur atom from the aforementioned surface to create a double vacancy. This leads to a highly unsaturated site with one tetracoordinated molybdenum atom and two pentacoordinated ones (Fig. 2c). The creation energy of site 2 starting from site 1 configuration is computed to be 2.1 eV, leading to an energy of 3.4 eV above the most stable structure. Finally, the last site (site 3) is located on the sulfur edge. It is obtained by removing three sulfur atoms from the saturated surface as shown in Fig. 2d. The creation of this site requires 2.9 eV. This surface presents highly unsaturated molybdenum atoms (penta-, tetra-, and tricoordinated). This high unsaturation is partly balanced by a strong Mo–Mo interaction and the creation of a S–S bond that stabilizes the whole system. Indeed, the distance between the two molybdenum atoms decreases from 3.16 to 2.23 Å and the S–S distance of 2.16 Å (vs 3.06 Å in the stable surface) indicates that a chemical bond has been formed between the two S atoms.

A more detailed analysis of these creation energies could be obtained by taking into account temperature and pressure effects through the introduction of gas-phase chemical potential corrections as shown in previous publications [17,34]. This thermodynamical treatment will not be applied in this paper, however, the energy required to create the CUS will be lowered by chemical potential contributions of the gas phase as the surrounding atmosphere is highly reductive. The vacancy creation energies obtained here can thus be considered as the upper limit.

4. Adsorption of molecules

We have considered three possible adsorption modes on all the selected potentially active sites:

- Adsorption in a η^1 geometry, the interaction between the molecule and the surface is made through the sulfur atom of the molecule;
- adsorption (η^3 or η^6) through one of the benzene rings of the molecule;
- adsorption (η^3 or η^5) through the thiophene ring of the molecule.

Adsorption involving more than one ring as proposed in [22] is impossible in our model due to the higher sulfur coverage of the surfaces. In order to evaluate the effect of DBT and DMDBT aromaticity, the adsorption of benzothiophene (BT) and 4-methylbenzothiophene (MBT) was also considered [21]. The same adsorption modes are also possible for BT and MBT. Adsorption energies of all these molecules on the different sites are compiled in Table 1. The adsorption energies are computed as the difference between the electronic energies (no ZPE corrections). A positive adsorption energy means that the system is more stable in the adsorbed state.

4.1. Adsorption on site 1 and site 3

On sites 1 and 3, η^1 adsorption is imposed by the geometry of the active site. BT and DBT adsorption geometries are quite similar, although the adsorption energy of the lat-

Table 1
Adsorption energies (eV) for the different molecules on different sites

Site	Adsorption mode	BT[a]	MBT[a]	DBT	DMDBT[b]
Site 1	η^1	0.5	0.4	0.7	
Site 2	η^1	1.1	0.9	1.3	0.3
	Thiophene	1.5	1.5	0.6	0.7
	Benzene	1.2	1.2	1.2	1.2
Site 3	η^1	0.8	0.4	0.5	

[a] Taken from Ref. [21].
[b] DMDBT adsorption is impossible on sites 1 and 3.

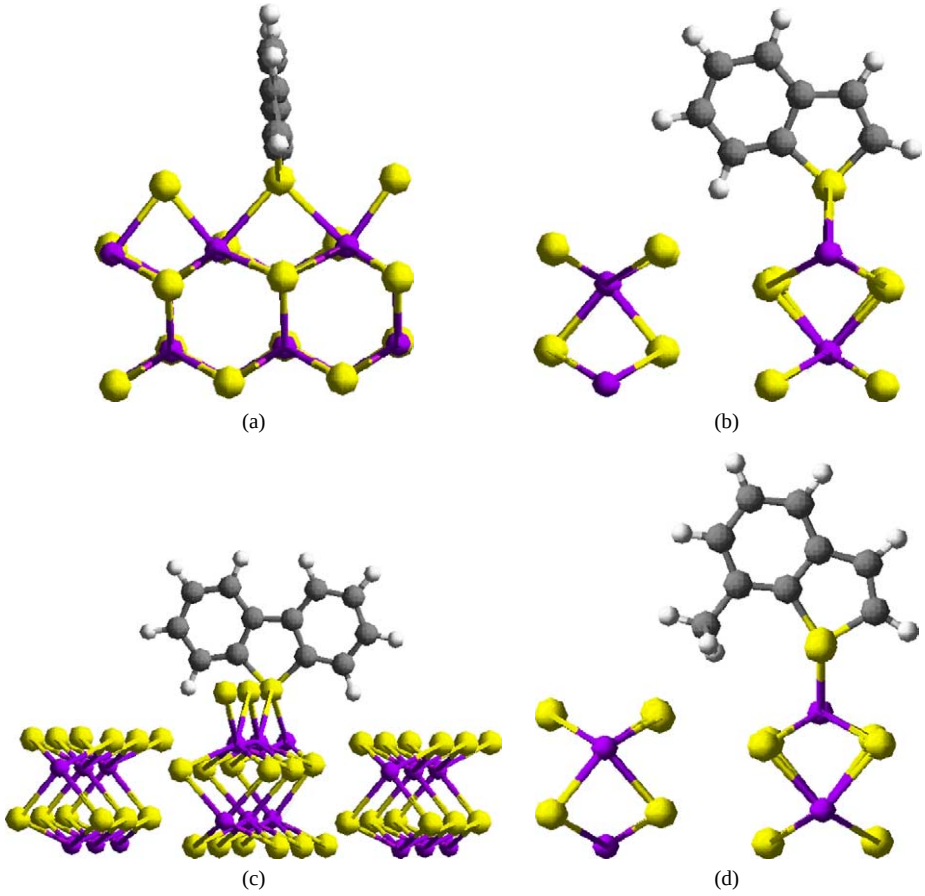

Fig. 3. Adsorption on site 1. (a) BT side view. (b) BT front view. (c) MBT front view. (d) DBT front view.

ter is slightly higher. The molecules are adsorbed in a plane perpendicular to the MoS_2 layer, the sulfur atom being in a bridging position between the two unsaturated molybdenum atoms. The higher adsorption energy for DBT is probably due to the fact that the sulfur lone pairs are less participating in the π system of DBT than of BT.

The presence of the methyl groups in DMDBT makes the η^1 adsorption of this molecule impossible. The steric repulsion between those groups and the surface is too large for the sulfur atom to be close enough to the surface to interact with the unsaturated molybdenum atoms. The effect of the methyl group on the adsorption energies for BT derivatives is much smaller. The adsorption geometries shown in Fig. 3 give a quite simple explanation of this phenomenon. It can be seen (Fig. 3d) that the MBT molecule is tilted to reduce steric interaction between the methyl group and the surface. This geometrical modification does not induce an important change in the electronic interaction between the molecule and the surface, but does significantly reduce the steric repulsion. The adsorption energy is thus almost the same for BT and MBT on site 1. Of course, such a tilt of the molecule is impossible for DMDBT as there is a methyl group on the other side of the molecule as well.

The situation on site 3 is slightly different since the methyl group of MBT remains too close to the surface even after tilting as shown on Fig. 4b. The MBT adsorption energy is thus two times smaller than BT one. This surface steric hindrance is also shown by the smaller adsorption energy found for DBT compared to BT. Although the DBT adsorption energy is higher than that of BT on site 1, it is smaller on site 3. The lower adsorption energy is mainly due to a steric repulsion between the two phenyl groups of the molecule and the surface. As could be expected from these results, DMDBT adsorption on site 3 is impossible.

Finally, it is worth pointing out that adsorption on site 3 seems to activate the molecule more strongly than adsorption on site 1. The C–S distances, which are good indicators of the activation of the molecule upon adsorption are compiled in Table 2. The numbering of the atoms of the molecules is shown on Fig. 5. Comparing Tables 1 and 2, one notes that there is no straight correlation between the adsorption energy and the activation of the molecule. Indeed, DBT adsorption on site 3 is weaker than on site 1, although the C–S bond is longer than when the adsorption proceeds on site 1. This effect is also observed for MBT adsorption and to a smaller extent for BT. In fact, the adsorption can be considered as the sum of an electronic effect, which leads to the activation of the molecule, and a steric repulsion that may significantly reduce the adsorption energy without changing the molecular activation. From this point of view, the electronic contribu-

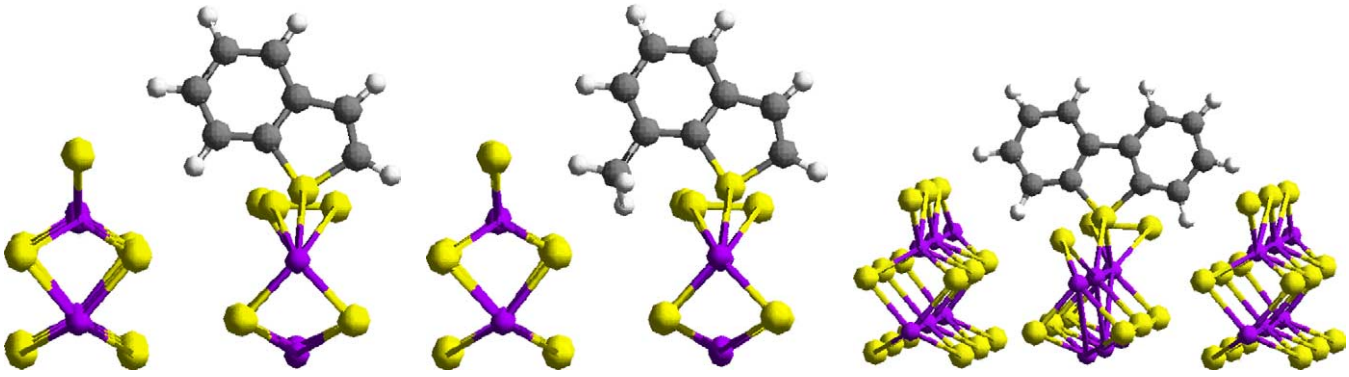

(a) (b) (c)

Fig. 4. Adsorption on site 3. (a) BT adsorption. (b) MBT adsorption. (c) DBT adsorption.

Table 2
C–S bond length (Å) in the free and η^1-adsorbed molecules on different sites

	BT		MBT		DBT	DMDBT[a]
	C_6–S	C_{4a}–S	C_6–S	C_{4a}–S	C_{4a}–S	C_{4a}–S
Free	1.73	1.74	1.73	1.74	1.75	1.75
Site 1	1.74	1.74	1.74	1.74	1.79	
Site 2	1.76	1.75	1.76	1.75	1.79	1.75
Site 3	1.77	1.80	1.76	1.78	1.81	

[a] DMDBT adsorption is impossible on sites 1 and 3.

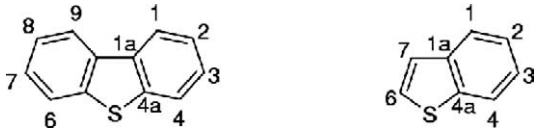

Fig. 5. Atom numbers in BT and DBT derivatives.

tion to the adsorption on site 3 is higher than on site 1, but the steric repulsion is also more important. All this is in agreement with the higher unsaturation of the molybdenum atoms on site 3, leading to a more important electronic contribution, and the fact that the molybdenum atoms on the sulfur edge are deeper inside the surface, inducing a higher steric repulsion upon adsorption.

4.2. Adsorption on site 2

The situation is more complex on site 2 as the three adsorption modes are possible for all the molecules we have considered as shown in Table 1. Considering η^1 adsorption first, we see that the influence of the methyl group is still very important. MBT adsorption is 0.2 eV weaker than BT adsorption and the adsorption geometry is modified similarly as on sites 1 and site 3. The steric repulsion between the methyl groups and the surface is much stronger with DMDBT and induces a strong decrease of the adsorption energy of DMDBT relative to DBT. In fact, the adsorption geometry is not the same for the two molecules. DBT adsorbs with its sulfur atom in a bridging position between two molybdenum atoms (Fig. 6b). The distances between the sulfur of DBT atoms and the five- and four-coordinated molybdenum atoms are 2.49 and 2.44 Å, respectively. The interaction between DMDBT and the surface proceeds only between the sulfur atom of the molecule and a four-coordinated molybdenum atom (Fig. 6a). The distance between them is 2.83 Å to reduce the steric interaction between the methyl groups and the surface. Hence this interaction is a weak physisorption, very different from the strong chemisorption of DBT on the same surface. This is confirmed by the analysis of the C–S distance in the two adsorbed molecules re-

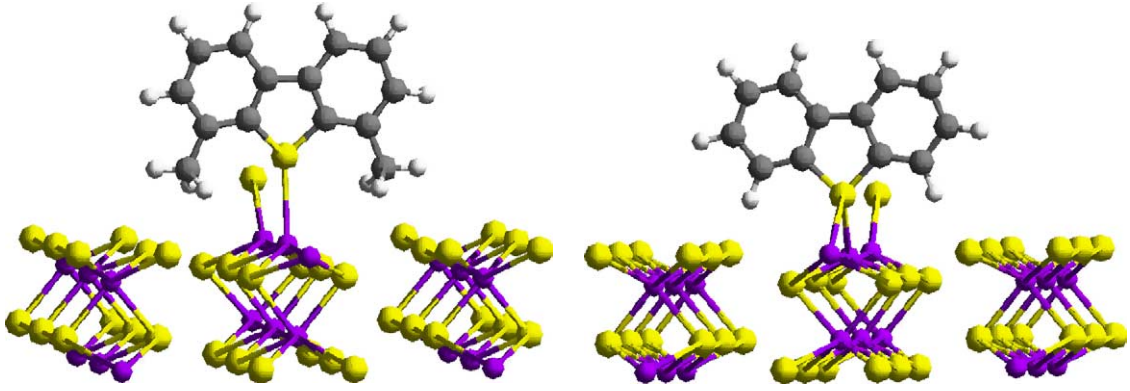

(a) (b)

Fig. 6. DBT and DMDBT adsorbed on site 2. (a) DBT. (b) DMDBT.

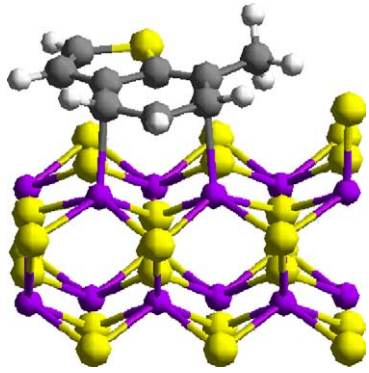

Fig. 7. MBT adsorbed on site 2 through its benzene ring.

ported in Table 2. There is a significant increase of the bond length for DBT, while for DMDBT the C–S bond is basically unaffected by the adsorption.

Considering now the other adsorption modes on site 2, Table 1 clearly shows that, whatever the molecule, the methyl groups have almost no influence on the adsorption energies when the main interaction is between the thiophene ring or the benzene ring and the surface ("flat" adsorption). Upon adsorption through the thiophene ring, the methyl group is pointing in a direction where there are no sulfur atoms. In the case of benzene ring adsorption, only three carbon atoms are in direct interaction with surface molybdenum atoms. Various orientations of the molecule relative to the surface are thus possible. The one minimizing the steric repulsion between the methyl groups of the molecule and the sulfur atom remaining on the surface is shown on Fig. 7.

Another interesting feature is that there is almost no difference between BT and DBT when the adsorption proceeds through the benzene ring, whereas the BT adsorption energy is 0.8 eV higher than for DBT when the adsorption proceeds through the thiophene ring. From the adsorption geometries shown on Fig. 7 and the bond distances compiled on Table 3, it can be seen that, when the adsorption proceeds through the benzene ring, the thiophene ring of the molecules is almost not affected. In contrast, when the adsorption proceeds through the thiophene ring, the BT thiophene ring is highly distorted (Fig. 8). The bond distances in the adsorbed molecule confirm that the thiophene ring cannot be considered

Table 3
Selected bond length (Å) in the free and adsorbed molecules for a thiophene or benzene adsorption on site 2

Molecule	Bond	Free	Adsorption	
			Thiophene	Benzene
BT	C_6–S	1.73	1.80	1.73
	C_{4a}–S	1.74	1.77	1.74
	C_6–C_7	1.38	1.47	1.40
	C_{1a}–C_{4a}	1.43	1.43	1.43
MBT	C_6–S	1.73	1.79	1.73
	C_{4a}–S	1.74	1.77	1.74
	C_6–C_7	1.38	1.46	1.40
	C_{1a}–C_{4a}	1.43	1.43	1.43
DBT	C_{4a}–S	1.75	1.78	1.75
	C_{1a}–C_{4a}	1.43	1.45	1.43
DMDBT	C_{4a}–S	1.75	1.78	1.75
	C_{1a}–C_{4a}	1.43	1.45	1.43

See Fig. 5 for the atom numbering.

aromatic any more. The C_6–C_7 bond is not even a double bond as its length (1.47 Å) is between a single and a double C–C bond. On the other hand the C_{1a}–C_{4a} bond is not affected by the adsorption. In other words, thiophene adsorption implies a rupture of aromaticity of the thiophene ring without affecting the benzene ring. Once again, only one ring is affected by the adsorption.

In the case of DBT, such an adsorption would imply the loss of aromaticity of two rings of the molecule: the thiophene ring and one of the benzene rings. Indeed the interaction between the molecule and the metal atom of the surface is not strong enough to balance and overcome the dearomatization of two aromatic rings. The adsorption energies of DBT and DMDBT through the thiophene ring are thus far smaller and this adsorption mode could be better described as an interaction between the sulfur atom of the thiophene ring and the surface.

The results of these important electronic effects are that, contrary to benzothiophene or thiophene derivatives [19,20], for which thiophene adsorption is dominant, the most favored DBT adsorption mode will be η^1(S) or benzene adsorption. This is a major difference between small model compounds and real refractory molecules. In the case of

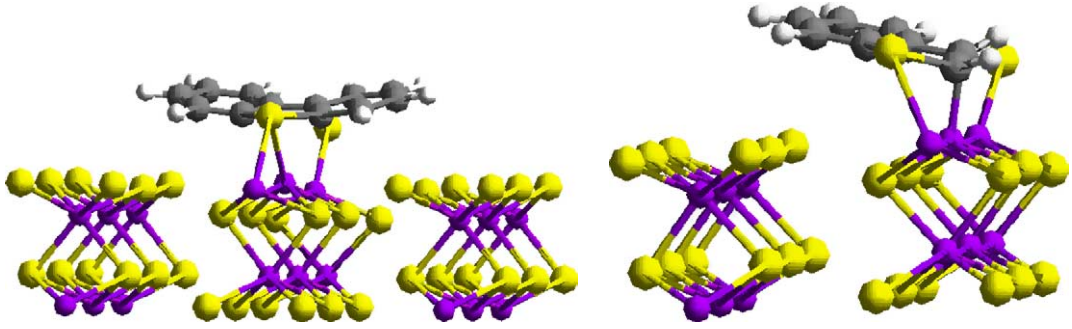

(a) (b)

Fig. 8. BT and DBT adsorbed on site 2 through the thiophene ring.

DMDBT, the conjunction of electronic effects that penalize adsorption through the thiophene ring, and steric effects that rule out η^1(S) adsorption, makes the adsorption through the benzene ring the only possible adsorption mode.

5. Influence of stacking defects on the adsorption of the molecules

In order to determine the origin of the steric interaction, we have investigated defects in the stacking of the active phase. We choose to investigate the effects of stacking faults only for sites 1 and 3 as steric hindrance is much more important on these sites that impose η^1 adsorption of the molecules. This point should be less important on site 2 as it allows flat adsorption where there is virtually no steric repulsion between the surface and the molecule.

Sites 1b and 3b are derived from site 1 and 3 by cutting the upper MoS_2 rows of the neighboring layers as shown in Fig. 9. Such defective sites allow us to take into account stacking faults in the active phase. They can also mimic a vertical (edge bonded) single MoS_2 layer, the presence of which has been observed on model catalysts [35,36]. In the case of real catalysts, MoS_2 monolayers have been observed [37,38] but the orientation of the nanocrystallite is reported to be dependent on the faces exposed by the support [39]. Our model cannot mimic the situation where the MoS_2 layers are flat on the support (basal bonded), in which steric repulsion between the adsorbed molecules and the support would probably be the dominating parameter.

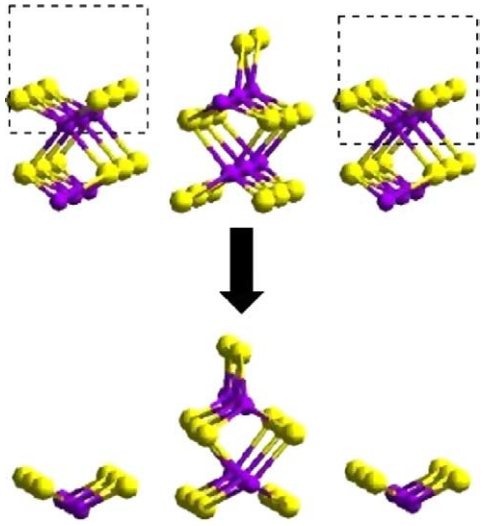

Fig. 9. Schematic representation of the creation of a stacking fault.

Table 4
Adsorption energies (eV) for DBT and DMDBT on different sites

Site	DBT	DMDBT
Site 1	0.7	–
Site 1b	0.7	–
Site 3	0.5	–
Site 3b	0.9	0.7

Adsorption energies for all molecules on both sites are compiled in Table 4 where adsorption energies on sites 1 and 3 (without stacking defects) have been included for the sake of comparison.

It can be seen that DMDBT adsorption on the metallic edge (site 1b) is still impossible even though steric interaction with the neighboring layers has been completely removed. This shows that the steric repulsion between the DMDBT methyl groups and the surface comes from the sulfur atoms of the layer where the adsorption takes place (or does not take place) itself as shown on Fig. 10.

On the sulfur edge (site 3b), the situation is quite different as DMDBT η^1 adsorption is made possible by the creation of stacking defects and its adsorption energy is almost the same as that of DBT. The reason for this difference between the two edges of the MoS_2(100) surface is straightforward when looking at the surface geometry. On the molybdenum edge, the sulfur atoms of the first sublayer of the surface are located between the two molybdenum atoms that interact with the molecule, just where the methyl groups are pointing upon adsorption (Fig. 10). On the sulfur edge, on the other hand, the sulfur atoms of the first sublayer are located

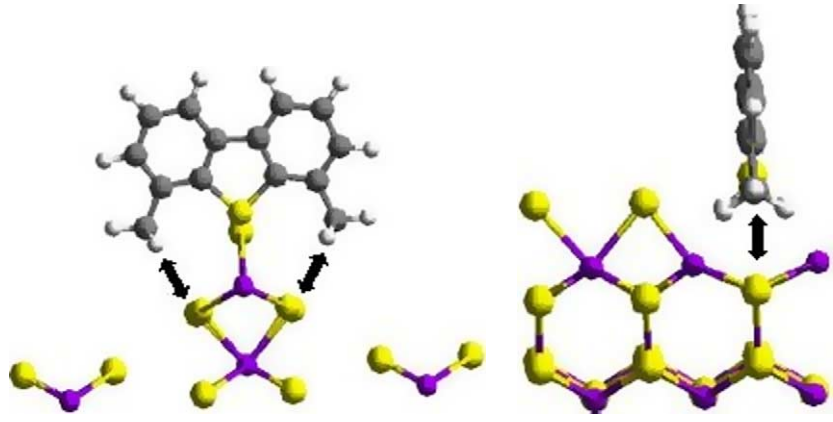

(a) (b)

Fig. 10. DMDBT on site 1 with a stacking fault. The arrows indicate the steric repulsion. (a) Front view. (b) Side view.

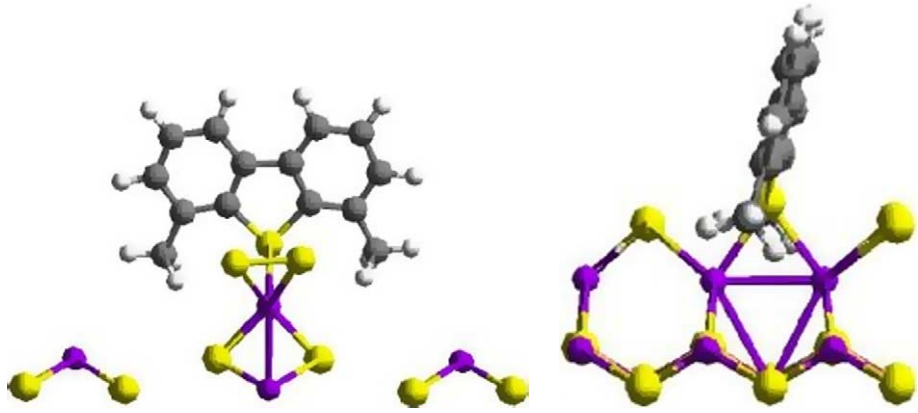

(a) (b)

Fig. 11. DMDBT adsorbed on site 3 with a stacking default. (a) Front view. (b) Side view.

just under the molybdenum atoms and the region between the molybdenum atoms is free (Fig. 11). The adsorption can then take place and, as there are no more steric interactions between the molecule and the neighboring layers (thanks to the presence of stacking faults), its energy is quite high. The steric repulsion in the case of the sulfur edge is thus almost completely removed by the stacking faults. The adsorption of the molecules on stacking defects also shows that steric interaction between DBT and the neighboring layers is quite important in the case of the adsorption on site 3. Indeed, the creation of the defect induces an increase of DBT adsorption energy of 0.4 eV. The activation of bonds upon adsorption of these sites is similar to the ones observed on the sites without stacking defects.

6. Discussion

On the basis of these results, we can propose an interpretation of the experimental results on the activity of unpromoted MoS_2 catalysts toward hydrodesulfurization even though the results reported by different teams are still quite controversial.

Farag et al. [40] concluded from a study of different unsupported molybdenum sulfide catalysts that there are two different active sites involved in the HDS activity of DBT. One is active in the hydrogenation reactions, the other one in hydrogenolysis. Furthermore, they found that the selectivity is influenced by the number of stacked MoS_2 layers (N) as previously reported by Daage and Chianelli [41] but not exactly in the same way. Daage and Chianelli reported a linear increase of the DDS/HYD ratio with an increase of the number of stacked layers over the whole range of N, whereas Farag et al. reported two different zones of N. In the first one ($N < 5$), the DDS/HYD ratio decreases when N is increasing, whereas in the second one ($N > 5$), the DDS/HYD ratio increases with N. Although these results are quite confusing, they show that the MoS_2 layer stacking is certainly playing an important role in the HDS activity and both groups agree that two different sites are required to model the whole HDS reaction pathway. Hensen et al. [38] reported that DBT HDS activity is influenced by the stacking degree of the molybdenum sulfide particles obtained using different supports. The DDS activity is always five times larger than the HYD one even with an average stacking between 1 and 3. According to the rim-edge model of Daage and Chianelli, such a morphology should result in strongly hydrogenative catalysts.

The DDS/HYD ratio is found between 65/35 and 35/65 by Orozco and Vrinat [42] depending on the nature of the support. Here again, this could be an effect of the active phase morphology, although it is not documented in the paper. These authors also show that the molar ratio of H_2S in the surrounding atmosphere has an inhibiting effect on the overall conversion (certainly related to the number of CUS present at the surface of the active phase), but also as a dramatic effect on the selectivity. Unfortunately, those teams do no report any data on DMDBT HDS on unpromoted molybdenum sulfide.

Hermann et al. [43] studied the activity of bulk MoS_2 toward DBT and DMDBT hydrodesulfurization. DBT HDS is performed under a pressure of 50 atm (38 atm of H_2 and 0.2 atm of H_2S) at 300 °C and the temperature required to obtain a similar conversion with DMDBT is 320 °C, demonstrating the well-known difficulty in desulfurizing dibenzothiophene derivatives alkylated in the 4 and 6 positions. They report a product distribution of less than 20% BP and more than 80% CHB for DBT HDS. They only detect traces of ring-hydrogenated but not desulfurized molecules, indicating that C–S bond hydrogenolysis is very fast once one of the benzene ring has been hydrogenated. For DMDBT, they find around 20% DMBP, 40% DMCHB, and 40% ring-hydrogenated but not desulfurized molecules, indicating that the steric problems encountered in the case of DMDBT HDS are not solved by the hydrogenation of one of its benzene rings.

Approximately at the same time Bataille et al. [44] reported a detailed study of the HDS of DBT and DMDBT on both promoted and unpromoted supported MoS_2. For the nonpromoted catalyst, they observe that the DBT and DMDBT conversions are quite similar at 340 °C under a to-

tal pressure of 40 atm (30 atm of H_2 and 0.5 atm of H_2S), although, if only the desulfurized product molecules are taken into account, DBT is much more reactive than DMDBT. Indeed, most of the converted DMDBT molecules are not desulfurized but hydrogenated. For DBT, they find 22% BP resulting from the DDS route, 60% ring-hydrogenated but not desulfurized molecules, and 18% CHB. For DMDBT they find only 8% DMBP resulting from the DDS route, 86% ring-hydrogenated but not desulfurized molecules, and 5% DMCHB.

Although unambiguous conclusions are difficult to draw from all these studies, maybe because of the discrepancies between the reaction conditions, all authors seem to agree on a few points. First, the degree of stacking of the active phase has a crucial influence on the selectivity. It should be pointed out that different degrees of stacking are obtained by a variation of the preparation methods, support, or post-treatment and all those parameters surely affect the stacking *quality* and the overall morphology of the active phase as well as the number of stacked layers. Second, there is no significant difference between DBT and DMDBT toward hydrogenation over unpromoted molybdenum sulfide. Finally, the hydrogenolysis of the C–S bond in methylated derivatives is more difficult than in non-methylated ones. This difference is not restricted to DBT and DMDBT but also applies for the hydrogenated intermediates.

It seems fair to assume that the hydrogenation route starts with the benzene ring adsorption. The hydrogenation pathway would then start by the adsorption of both DBT and DMDBT on the molybdenum edge (site 2). The adsorption energies and geometries are similar for both molecules and this might explain that they behave in the same way toward hydrogenation. The DDS pathway could be related to the only η^1 adsorption mode that leads to a significant activation which is the adsorption on site 3 located on the sulfur edge. This adsorption mode is restricted to DBT and that might be the reason for the lower DDS contribution for DMDBT observed in [44]. The residual DDS observed for DMDBT would be related to the presence of stacking defects allowing its adsorption on the sulfur edge. The lower reactivity of hydrogenated intermediates of DMDBT in hydrogenolysis reactions (compared to hydrogenated derivatives of DBT) is, in our opinion, an indication that this reaction does not take place on the hydrogenation site. We propose that the hydrogenolysis site is the same for hydrogenated and non-hydrogenated molecules (i.e., a triple vacancy on the sulfur edge). Such a mechanism implies a desorption of the hydrogenated molecule that explains the detection of an important amount of hydrogenated intermediates. The lower reactivity of hydrogenated DMDBT intermediates would then be explained, as for DMDBT, by the small number of potential active sites.

The implication of two different active sites (one hydrogenation reactions, the other responsible for hydrogenolysis of the C–S bonds) is still a matter of controversy. Several authors have used this proposal for kinetic modeling [10,11,40], while some others propose that a single site is at the origin of both reactions [38,44,45]. Our results seem to support the former. Another evidence supporting the two sites approach is the inhibiting effect of H_2S. It is well known that H_2S inhibits the DDS more strongly than the HYD path [10,42,46]. This fact finds a nice explanation in our model as we have shown [17] that introduction of H_2S will change the sulfur coverage of the sulfur edge (and thus strongly affect the DDS in our model) and less importantly change the properties of the molybdenum edge (and thus less change the HYD within our model). A computation of the different reaction pathways is now being undertaken to validate or invalidate our suggestions based only on the study of the adsorption of the various molecules.

7. Conclusion

In summary, we showed that when only η^1 adsorption is possible (on site 1 and 3), DMDBT cannot adsorb on the surface of the active phase although BT, MBT and DBT can. When the vacancy is larger and allows all the possible adsorption modes, the most favored adsorption for BT and MBT is the one involving the thiophene ring, leading to a strong activation of the C–S and C_6–C_7 double bond. On the same vacancy, there is a competition between η^1(S) and benzene adsorption for DBT, and DMDBT will adsorb mainly through its benzene ring. The adsorption properties of the really refractory molecules (DBT and DMDBT) are very different from those of the model compounds BT and MBT. The main reason for this difference is the aromaticity of DBT and DMDBT that prevents the adsorption through the thiophene ring. In conjunction with steric hindrance, this aromaticity imposes adsorption of DMDBT by the benzene ring except on very specific sites (i.e., triple vacancy on the sulfur edge in the presence of stacking faults).

A direct correlation between adsorption geometries and energies with the reactivity of molecules is not straightforward but on the basis of the present results, we propose that the hydrogenative route proceeds via a benzene adsorption on the molybdenum edge of the MoS_2 crystallites whereas the direct desulfurization proceeds by η^1 adsorption on the sulfur edge.

Acknowledgments

This work has been performed within the Groupement de recherche européen *Dynamique moléculaire quantique appliquée à la catalyse*, a joint project of the Centre National de la Recherche Scientifique (CNRS), Institut Français du Pétrole (IFP), Universität Wien (UW), TOTAL and Technische Universiteit Eindhoven (TUE). The authors thank IDRIS/CNRS and CRI/USTL (partially funded by FEDER) for the allocation of CPU time.

References

[1] European directive 98/70/CE, 1998.
[2] H. Topsøe, B.S. Clausen, F.E. Massoth, Hydrotreating Catalysis, Science and Technology, Springer, Berlin, 1996.
[3] H. Topsøe, B.S. Clausen, R. Candia, C. Wivel, S. Morup, J. Catal. 68 (1981) 433.
[4] D.D. Whitehurst, T. Isoda, I. Mochida, Adv. Catal. 42 (1998) 5.
[5] B.C. Gates, H. Topsøe, Polyhedron 16 (1997) 3213.
[6] X. Ma, I. Mochida, Ind. Eng. Chem. Res. 33 (1994) 218.
[7] M.J. Girgis, B.C. Gates, Ind. Eng. Chem. Res. 30 (1991) 2021.
[8] G.H. Singhal, R.L. Espino, J.E. Sobel, G.A. Huff Jr., J. Catal. 67 (1981) 457.
[9] T.C. Ho, J.E. Sobel, J. Catal. 128 (1991) 581.
[10] V. Vanrysselberghe, G. Froment, Ind. Eng. Chem. Res. 35 (1996) 3311.
[11] V. Vanrysselberghe, R. Le Gall, G. Froment, Ind. Eng. Chem. Res. 37 (1998) 1235.
[12] V. Lamure-Meille, E. Schulz, M. Lemaire, M. Vrinat, Appl. Catal. A 131 (1995) 143.
[13] S. Kasztelan, H. Toulhoat, J. Grimblot, J.-P. Bonnelle, Appl. Catal. 13 (1984) 127.
[14] P. Raybaud, G. Kresse, J. Hafner, H. Toulhoat, Surf. Sci. 407 (1998) 237.
[15] L.S. Byskov, J.K. Norskov, B.S. Clausen, H. Topsøe, J. Catal. 187 (1999) 109.
[16] P. Raybaud, G. Kresse, J. Hafner, S. Kasztelan, H. Toulhoat, J. Catal. 190 (2000) 128.
[17] S. Cristol, J.-F. Paul, E. Payen, D. Bougeard, F. Hutschka, S. Clémendot, J. Phys. Chem. B 104 (2000) 11220.
[18] S. Cristol, J.-F. Paul, E. Payen, D. Bougeard, F. Hutschka, S. Clémendot, J. Phys. Chem. B 106 (2002) 5659.
[19] P. Raybaud, G. Kresse, J. Hafner, H. Toulhoat, Phys. Rev. Lett. 80 (1998) 1481.
[20] H. Orita, K. Uchida, N. Itoh, J. Mol. Catal. A 193 (2003) 197.
[21] S. Cristol, J.-F. Paul, E. Payen, D. Bougeard, F. Hutschka, J. Hafner, Stud. Surf. Sci. Catal. 128 (1999) 327.
[22] H. Yang, C. Fairbridge, Z. Ring, Energy Fuels 17 (2003) 387.
[23] G. Plazenet, S. Cristol, J.-F. Paul, E. Payen, J. Lynch, Phys. Chem. Chem. Phys. 3 (2001) 246.
[24] A. Travert, C. Dujardin, F. Maugé, S. Cristol, J.-F. Paul, E. Payen, D. Bougeard, Catal. Today 70 (2001) 255.
[25] G. Kresse, J. Hafner, Phys. Rev. B 47 (1993) 558.
[26] G. Kresse, J. Hafner, Phys. Rev. B 49 (1994) 14221.
[27] G. Kresse, J. Furthmüller, Phys. Rev. B 47 (1996) 558.
[28] G. Kresse, J. Furthmüller, Comput. Mater. Sci. 6 (1996) 15.
[29] N.D. Mermin, Phys. Rev. 137 (1965) A1141.
[30] D. Vanderbilt, Phys. Rev. B 41 (1990) 7892.
[31] G. Kresse, J. Hafner, J. Phys.: Condens. Matter 6 (1994) 8245.
[32] J.P. Perdew, A. Zunger, Phys. Rev. B 23 (1981) 5048.
[33] J.P. Perdew, J.A. Chevary, S.H. Vosko, K.A. Jackson, M.R. Pederson, D.J. Singh, C. Frolais, Phys. Rev. B 46 (1992) 6671.
[34] P. Raybaud, G. Kresse, J. Hafner, S. Kasztelan, H. Toulhoat, J. Catal. 189 (2000) 129.
[35] Y. Araki, K. Honna, H. Shimada J. Catal. 207 (2002) 361.
[36] Y. Sakashita, T. Yoneda, J. Catal. 185 (1999) 487.
[37] E. Payen, R. Hubaut, S. Kasztelan, O. Poulet, J. Grimblot, J. Catal. 147 (1994) 123.
[38] E.J.M. Hensen, P.J. Kooyman, Y. van der Meer, A.M. van der Kraan, V.H.J. de Beer, J.A.R. van Veen, R.A. van Santen, J. Catal. 199 (2001) 224.
[39] Y. Sakashita, Y. Araki, H. Shimada, Appl. Catal. A 215 (2001) 101.
[40] H. Farag, K. Sakanishi, M. Kouzu, A. Matsumura, Y. Sugimoto, I. Saito, J. Mol. Catal. A: Chem. 206 (2003) 399.
[41] M. Daage, R.R. Chianelli, J. Catal. 149 (1994) 414.
[42] E. Olguin Orozco, M. Vrinat, Appl. Catal. A 170 (1998) 195.
[43] N. Hermann, M. Brorson, H. Topsøe, Catal. Lett. 65 (2000) 169.
[44] F. Bataille, J.L. Lemberton, P. Michaud, G. Pérot, M. Vrinat, M. Lemaire, E. Schulz, M. Breysse, S. Kasztelan, J. Catal. 191 (2000) 409.
[45] V. Meille, E. Schulz, M. Lemaire, M. Vrinat, J. Catal. 170 (1997) 29.
[46] T. Kabe, W. Qian, A. Ishihara, Catal. Today 39 (1997) 3.